

## Article

# Constructing artificial features with Grammatical Evolution for earthquake prediction

Constantina Kopitsa<sup>1</sup>, Glykeria Kyrou<sup>2</sup>, Vasileios Charilogis<sup>3</sup> and Ioannis G. Tsoulos<sup>4,\*</sup>

<sup>1</sup> Department of Informatics and Telecommunications. University of Ioannina, Greece k.kopitsa@uoi.gr

<sup>2</sup> Department of Informatics and Telecommunications. University of Ioannina, Greece g.kyrou@uoi.gr

<sup>3</sup> Department of Informatics and Telecommunications. University of Ioannina, Greece v.charilog@uoi.gr

<sup>4</sup> Department of Informatics and Telecommunications. University of Ioannina, Greece itsoulos@uoi.gr

\* Correspondence: itsoulos@uoi.gr

## Abstract

Earthquakes are the result of the dynamic processes occurring beneath the Earth's crust specifically, the movement and interaction of tectonic / lithospheric plates. When one plate shifts relative to another, stress accumulates and is eventually released as seismic energy. This process is continuous and unstoppable. This phenomenon is well recognized in the Mediterranean region, where significant seismic activity arises from the northward convergence (4-10 mm per year) of the African plate relative to the Eurasian plate along a complex plate boundary. Consequently, our research will focus on the Mediterranean region, specifically examining seismic activity from 1990 - 2015 within the latitude range of 33-44° and longitude range of 17-44°. These geographical coordinates encompass 28 seismic zones, with the most active areas being Turkey and Greece. In this paper we applied Grammatical Evolution for artificial feature construction in earthquake prediction, evaluated against machine learning approaches including MLP(GEN), MLP(PSO), SVM, and NNC. Experiments showed that Feature Construction (FC) achieved the best performance, with a mean error of 9.05% and overall accuracy of 91%, outperforming SVM. Further analysis revealed that a single constructed feature ( $N_f = 1$ ) yielded the lowest average error (8.21%), while varying the number of generations indicated that  $N_g = 200$  provided an effective balance between computational cost and predictive accuracy. These findings confirm the efficiency of FC in enhancing earthquake prediction models through artificial feature construction. Our results, as will be discussed in greater detail within the research, yield an average error of approximately 9%, corresponding to an overall accuracy of 91%.

Received:

Revised:

Accepted:

Published:

Citation: Kopitsa, C.; Kyrou, G.; Charilogis, V.; Tsoulos, I.G..

Constructing artificial features with Grammatical Evolution for earthquake prediction. *Journal Not Specified* **2025**, *1*,

0. <https://doi.org/>

Copyright: © 2026 by the authors.

Submitted to *Journal Not Specified* for possible open access publication under the terms and conditions of the Creative Commons Attribution (CC BY) license (<https://creativecommons.org/licenses/by/4.0/>).

**Keywords:** Earthquakes; Machine learning; Neural networks; Grammatical Evolution; Feature Construction

## 1. Introduction

When entering the single keyword "earthquakes" into Google Scholar, more than 3,910,000 results are retrieved, demonstrating the intense interest that exists in the field of seismology. Thanks to these studies and investigations, which evolve from an initial idea or theory into practical applications, it can be stated with confidence that humanity is now capable of achieving timely early warning before seismic events occur. Consequently, the pursuit of sustainability strengthens our resilience against seismic phenomena. This has been achieved through the implementation of early warning systems established across the globe, particularly in technologically advanced countries that are also seismically vulnerable regions. For this purpose, the UN Disaster Risk Reduction was established, which

is “aimed at preventing new and reducing existing disaster risk and managing residual risk, all of which contribute to strengthening resilience and therefore to the achievement of sustainable development” [1]. An early achievement of Disaster Risk Reduction took place in Japan in 1960, when seismic sensors were installed along the railway infrastructure to ensure the automatic immobilization of trains [2]. The Japanese UrEDAS (Urgent Earthquake Detection and Alarm System) has been described as the “grandfather” of earthquake early warning systems in general, and of onsite warning systems in particular [3]. Since then, techniques and methods have advanced through technological progress. The next achievement in early earthquake warning was accomplished in Mexico in 1989 with the establishment of the Seismic Alert System (SAS) [4]. In 2006, Japan launched the Earthquake Early Warning system initially for a limited audience and subsequently for the general public, in order to ensure the effectiveness of EEW in disaster mitigation [5]. This allows an earthquake warning to be disseminated between several seconds and up to one minute prior to the occurrence of the event [6]. In Bucharest, Romania, an earthquake warning system, in 1999, was also developed, providing a preparation window of 25 seconds [7]. Also in Istanbul, in preparation for the anticipated earthquake, an early warning system was implemented in 2002 [8]. In Southern Europe, at the University of Naples in Italy, a software model called PRESTo (PRobabilistic and Evolutionary early warning SysTem) was developed, designed to estimates of earthquake location and size within 5-6 seconds [9]. Furthermore, the United States, through the U.S. Geological Survey, has established its own earthquake warning system. Since 2016, the ShakeAlert system has been operational along the West Coast [10,11]. Subsequently, a map is presented in Figure 1, illustrating Earthquake Early Warning Systems worldwide, with colors indicating the operational status of each system, provided in [12]. Purple denotes operative systems that provide warnings to the public, black represents systems currently undergoing real-time testing, and gray is used for countries where feasibility studies are still in progress.

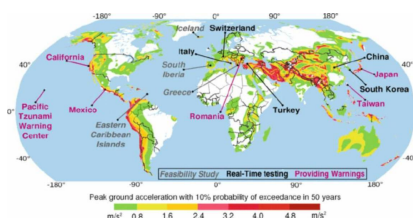


**Figure 1.** The map shows Earthquakes Early Warning Systems around the World

Within this framework, it is important to highlight that in recent years considerable emphasis has been placed on the advancement of diverse models for the early detection of seismic events, which have become available to the wider public through mobile applications, television broadcasts, and radio communication [13]. The primary function of Android applications is that, once an earthquake is detected, an alert is transmitted to all smartphones located within the affected area. Provided that the user is not in close proximity to the epicenter, the notification can be received in advance, allowing sufficient time to take protective action before the destructive seismic waves arrive [14–17]. By harnessing technology as an ally against natural disasters, humanity can move beyond the devastating consequences of major earthquakes, such as the 2004 Indian Ocean event with more than 220,000 fatalities, the 2011 Tōhoku earthquake in Japan with over 19,000 losses, and the 2023 Turkey-Syria earthquake with more than 43,000 deaths. Accordingly, resilience and sustainability for populations affected by seismic events encompass both physical and social infrastructures capable of withstanding earthquakes, while simultaneously safeguarding long-term well-being through disaster risk reduction, community preparedness, and equitable recovery.

Subsequently, we will proceed with the presentation of related studies alongside our own, which progressively enhance both our sustainability and our capacity for prevention against seismic phenomena. Housner, in 1964, concluded that artificial earthquakes constitute adequate representations of strong-motion events for structural analysis and may serve as standard ground motions in the design of engineering structures [18]. Adeli, in 2009, proposed a novel feature extraction technique, asserting that when combined with a selected Probabilistic Neural Network (PNN), it can yield reliable prediction outcomes for earthquakes with magnitudes ranging from 4.5 to 6.0 on the Richter scale [19]. Zhou, in 2012, introduced a robust feature extraction approach, the Log-Sigmoid Frequency Cepstral Coefficients (LSFCC), derived from the Mel Frequency Cepstral Coefficients (MFCC), for the classification of ground targets using geophones. Employing LSFCCs, the average classification accuracy for tracked and wheeled vehicles exceeds 89% across three distinct geographical settings, achieved with a single classifier trained in only one of these environments [20]. Martinez-Alvarez, in 2013, investigated the utilization of various seismicity indicators as inputs for artificial neural networks. The study proposes combining multiple indicators—previously shown to be effective across different seismic regions through the application of feature selection techniques [21]. Schmidt, in 2015, proposed an efficient and automated method for seismic feature extraction. The central concept of this approach is to interpret a two-dimensional seismic image as a function defined on the vertices of a carefully constructed underlying graph [22]. Narayananakumar, in 2016, extracted seismic features from a predetermined number of events preceding the main shock in order to perform earthquake prediction using the Backpropagation (BP) neural network technique [23]. Cortes, in 2016, sought to identify the parameters most effective for earthquake prediction. As various studies have employed different feature sets, the optimal selection of features appears to depend on the specific dataset used in constructing the model [24]. Asim, in 2018, developed a hybrid embedded feature selection approach designed to enhance the accuracy of earthquake prediction [25]. Chamberlain, in 2018, demonstrated that synthetic seismograms, when applied with matched-filter techniques, enable the detection of earthquakes even with limited prior knowledge of the source [26]. Okada, in 2018, employed observational data either by calibrating parameters within existing models or by deriving models and indicators directly from the data itself [27]. Lin, in 2018, employed the earthquake catalogue from 2000 to 2010, comprising events with a Richter magnitude (ML) of 5 and a depth of 300 km within the study area ( $21^{\circ}$ - $26^{\circ}$  N,  $119^{\circ}$ - $123^{\circ}$  E). This dataset was utilized as training input to develop the initial earthquake magnitude prediction backpropagation neural network (IEMPBPN) model, which was designed with two hidden layers [28]. Zhang, in 2019, proposed a precursory pattern-based feature extraction approach aimed at improving earthquake prediction performance. In this method, raw seismic data are initially segmented into fixed daily time intervals, with the magnitude of the largest earthquake within each interval designated as the main shock [29]. Rohas's, in 2019, paper reviewed the latest uses of artificial neural networks for automated seismic-data interpretation, focusing especially on earthquake detection and onset-time estimation [30]. Ali, in 2020, generated synthetic seismic data for a three-layer geological model and analyzed using Continuous Wavelet Transform (CWT) to identify seismic reflections in both the temporal and spatial domains [31]. Bamer, in 2021, demonstrated through comparison with several state-of-the-art studies, that the convolutional neural network autonomously learns to extract the pertinent input features and structural response behavior directly from complete time histories, rather than relying on a predefined set of manually selected intensity measures [32]. Wang, in 2023, reports that the accuracies of various AI models using the feature extraction dataset surpassed those obtained with the spectral amplitude dataset, demonstrating that the feature extraction approach more effectively emphasizes

the distinctions among different types of seismic events [33]. Ozkaya, in 2024, developed a novel feature engineering framework that integrates the Butterfly Pattern (BFPat), statistical measures, and wavelet packet decomposition (WPD) functions. The proposed model achieved an accuracy of 99.58% in earthquake detection and 93.13% in three-class wave classification [34]. Sinha's review, in 2025, offers valuable insights into cutting-edge techniques and emerging directions in feature engineering for seismic prediction, highlighting the importance of interdisciplinary collaboration in advancing earthquake forecasting and reducing seismic risk [35]. Mahmoud, in 2025, investigates the application of machine learning approaches to earthquake classification and prediction using synthetic seismic datasets [36].

In contrast to the aforementioned studies, this paper introduces a novel approach constructing artificial features with Grammatical Evolution [37] for earthquake prediction, marking the first application of this evolutionary technique in the field of seismology. While the method does not directly address a specific gap in the literature, the experiments demonstrated that feature construction achieved an overall accuracy of 91%, thereby contributing to the advancement of earthquake prediction research. We consider this contribution significant in enhancing the understanding of seismic phenomena and in highlighting the potential of Grammatical Evolution as a promising tool for feature engineering in geophysical datasets. In particular, the method of Grammatical Evolution can be considered as a genetic algorithm [38] with integer chromosomes. Each chromosome contains a series of production rules from the provided Backus-Naur form (BNF) grammar [39] of the underlying language and hence this method can create programs that belong to this language. This procedure have been used with success in various cases, such as data fitting problems [40,41], problems that appear in economics [42], computer security problems [43], problems related to water quality [44], problems appeared in medicine [45], evolutionary computation [46], hardware issues in data centers [47], solution of trigonometric problems [48], automatic composition of music [49], dynamic construction of neural networks [50,51], automatic construction of constant numbers [52], playing video games [53,54], problems regarding energy [55], combinatorial optimization [56], security issues [57], automatic construction of decision trees [58], problems in electronics [59], automatic construction of bounds for neural networks [60], construction of Radial Basis Function networks [61] etc. This research work focuses on the creation of artificial features from existing ones, aiming at two goals: on the one hand, it seeks to reduce the required information required for the correct classification of seismic data and on the other hand, it seeks to highlight the hidden nonlinear correlations that may exist between the existing features of the objective problem. In this way, a significant improvement in the classification of seismic data will be achieved.

Beyond the Grammatical Evolution approach proposed in this study, which achieved an accuracy of 91%, we will also provide a concise comparison with results from related research that has employed alternative machine learning techniques in the field of seismology. In the study by Adeli et al. [19] the PNN model demonstrated satisfactory predictive accuracy for earthquakes with magnitudes between 4.5 and 6.0, but its performance declined considerably for events exceeding magnitude 6.0. Zhou et al. [20] reported that the application of the Log-Sigmoid Frequency Cepstral Coefficients method achieved an average classification accuracy exceeding 89%. Narayananakumar et al. [23] investigated the prediction of moderate earthquakes (magnitude 3.0-5.8). While the seismometer recorded an event of magnitude 4.0, the BP-ANN model predicted magnitudes in the range of 3.0-5.0, achieving a success rate between 75% and 125%. According to Asim et al., [25] the SVR-HNN prediction model achieved its highest performance in Southern California, with MCC, R score, and accuracy values of 0.722, 0.623, and 90.6%, respectively. The Chilean region ranked second, yielding an MCC of 0.613, an R score of 0.603, and an accuracy of

84.9%. In contrast, the Hindu Kush region exhibited the lowest performance, with MCC, R score, and accuracy values of 0.600, 0.580, and 82.7%, respectively. Chamberlain et al. [26] reported that template-based detections produced 7,340 events, of which 3,577 were identified as duplicates, whereas the STA/LTA method yielded 682 detections over the same time interval. Lin et al. [28] reported that the average magnitude error in Taiwan was  $\Delta ML = \pm 0.3$ , while the training errors of the EEMPBPN model ( $<0.25$ ) remained below this average error threshold. Zhang et al. [29] demonstrated that the proposed method achieved prediction accuracies of 93.26% and 92.07% across the two datasets examined. Rojas et al. [30] reported recognition performance of approximately 99.2% for P-wave signals and 98.4% for pure noise. Ali et al. [31] conducted a statistical analysis using a 95% confidence interval for the normalized CWT coefficients of P-wave velocity, seismic trace, acoustic impedance, and synthetic seismic trace. Wang et al. [33] found that, in the model generalization evaluation, the two-class models trained on the 36-dimensional network-averaged dataset achieved test accuracies and F1-scores exceeding 90%. Ozkaya et al. [34] reported that their model achieved an accuracy of 99.58% in earthquake detection and 93.13% in three-class wave classification. While comparable studies have demonstrated strong performance, many of them are limited to specific regions of interest or focus on particular signal types such as acoustic wave detection. In contrast, the Grammatical Evolution approach presented here not only achieves competitive accuracy (91%) but also demonstrates broader applicability across diverse seismic datasets, thereby highlighting its potential as a more generalizable solution in earthquake event discrimination.

The rest of this manuscript is organized as follows: the used dataset and the incorporated methods used in the conducted experiments are outlined in section 2, the experimental results are shown and discussed in section 3 and finally a detailed discussion is provided in section 4.

## 2. Materials and Methods

In this section, a detailed presentation of the datasets used as well as the machine learning techniques used in the experiments performed will be provided.

### 2.1. The Dataset Employed

In this study, we made use of open data from the NSF Seismological Facility for the Earth Consortium (SAGE) available from <https://ds.iris.edu/> (accessed on 25 November 2025), which is a platform offering an interactive global map that facilitates both data visualization and the real-time extraction of datasets from the displayed geographic regions. The area defined by latitudes 33°-44° and longitudes 17°-44° covers 28 seismic zones, with Turkey and Greece identified as the most seismically active regions.

Regarding the 28 seismic zones listed in Table 1, these correspond to specific geographic coordinates (latitudes and longitudes) provided through the interactive seismic platform previously referenced. The platform grants direct access to these spatial data, ensuring that the delineation of the zones is both systematic and consistent with the established geospatial framework.

**Table 1.** Regions codes for the 28 seismic zones.

| Region                                   | Region Code |
|--|-------------|
| Turkey                                   | 1           |
| Crete Greece                             | 2           |
| Greece                                   | 3           |
| Dodecanese Islands, GREECE               | 4           |
| Ionian Sea                               | 5           |
| Aegean Sea                               | 6           |
| Southern Greece                          | 7           |
| GREECEALBANIA border region              | 8           |
| GREECEBULGARIA border region             | 9           |
| Cyprus region                            | 10          |
| Albania                                  | 11          |
| NORTHWESTERN Balkan Region               | 12          |
| Central Mediterranean sea                | 13          |
| Jordan Syria region                      | 14          |
| GEORGIA ARMENIA TURKEY<br>Border Region  | 15          |
| TURKEY IRAN border region                | 16          |
| Iraq                                     | 17          |
| Eastern Mediterranean sea                | 18          |
| NORTHWESTERN CAUCASUS                    | 19          |
| Black Sea                                | 20          |
| Romania                                  | 21          |
| Bulgaria                                 | 22          |
| Crimea Region Ukraine                    | 23          |
| ARMENIA AZERBAIJAN IRAN<br>border region | 24          |
| Adriatic sea                             | 25          |
| UKRAINE MOLDOVA RUSSIA<br>border region  | 26          |
| Southern Italy                           | 27          |
| IRAN IRAQ border region                  | 28          |

Furthermore, the selection of NSF data was driven by its advanced functionality and broad accessibility. Notably, it supports the download of up to 25,000 records per file, thereby streamlining the workflow and improving the efficiency of information retrieval. The region under investigation is presented in Figure 2. This image was retrieved from IRIS Earthquake Browser, in the following URL: <https://ds.iris.edu/ieb/index.html?format=text&nodata=404&starttime=2010-01-01&endtime=2010-12-31&orderby=time-desc&src=iris&limit=1000&maxlat=74.85&minlat=-7.26&maxlon=135.19&minlon=-97.36&zmm=3&mtn=ter>

**Figure 2.** The study area.

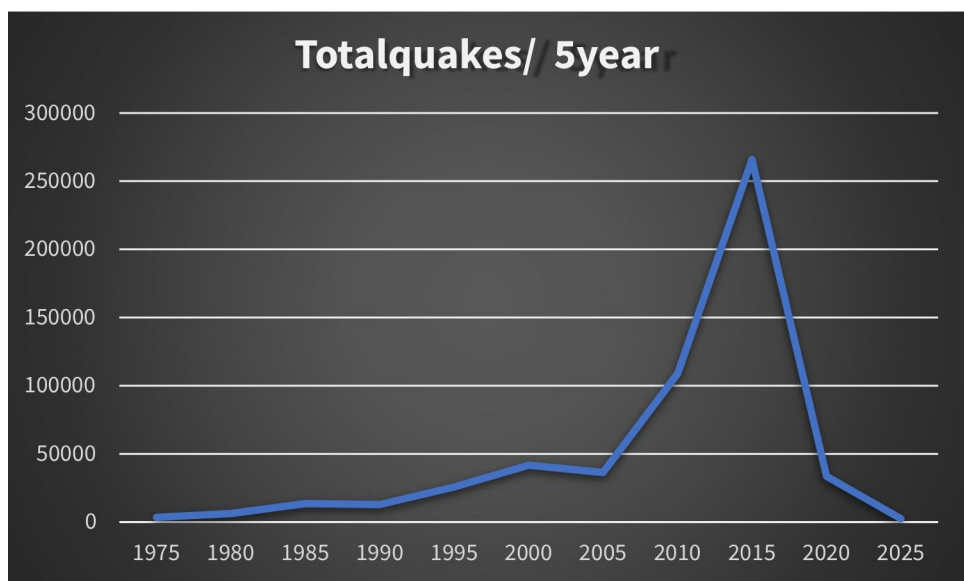
## 2.2. Dataset Description

We obtained and systematically analyzed 511,064 earthquake events from 1990 to 2015, as this time period is of particular scientific interest due to the surge in seismic activity, as also illustrated in the graph of Figure 3. Specifically, we selected this time period because it encompasses a wide range of earthquake magnitudes, which provides a diverse dataset

conducive to algorithm training and supports the construction of artificial features via Grammatical Evolution.

In the years under examination, earthquakes are distributed across all magnitude classes, exhibiting an almost ideal proportion consistent with the Gutenberg-Richter law [63]. For instance, within the first two five-year periods of our dataset, 2 events above magnitude 8.0, 3 events above magnitude 7.0, 19 events above magnitude 6.0, 165 events between 5.0-5.9, 3,048 events between 4.0-4.9, and 26,301 events between 3.0-3.9 were recorded, thereby confirming the expected logarithmic relationship between frequency and magnitude. Such a balanced and representative dataset further enhances the effectiveness of the Grammatical Evolution approach, as it provides a comprehensive distribution of seismic events across the full spectrum of magnitudes. Moreover, our analysis led us to the conclusion that the datasets from 1970-1989 and 2016-2025 lack the diversity observed in the dataset we selected. Specifically, classes 6 and 7 are entirely absent from the 1970-1989 records, while in the post-2016 data class 7 is missing and class 1 contains only a limited number of instances, namely 25.

**Figure 3.** Graphs seismic events from 1970 - 2025 (Area Study)



On the platform that provides us with the Interactive Earthquake Browser we employed coordinates spanning latitudes  $33^{\circ}$ - $44^{\circ}$  and longitudes  $17^{\circ}$ - $44^{\circ}$ , considered magnitude values from 1.0 to 10.0, and incorporated all available depths by default within the depth range. The raw dataset included the following variables: year, month, day, time, latitude (Lat), longitude (Lon), depth, magnitude, region, and timestamp. Accordingly, Table 2 provides a detailed overview of the raw dataset.

Subsequently, a preprocessing procedure was applied to the dataset. This included the identification of the lithospheric plate associated with each earthquake, to which a unique code was assigned. Furthermore, the months were categorized according to the four seasons, the days were grouped into ten-day intervals, and the time of occurrence was classified into four periods (morning, noon, afternoon, and night). The focal depth was divided into six categories. In addition, a new column was created to indicate, with a binary value (0 or 1), whether an earthquake had previously occurred in the same region during the same season. Finally, the dataset was merged with the Kp index, representing geomagnetic storm activity, which was further classified into six distinct categories. The final dataset was further processed, including the following: Year, Epoch Code, Day Code,

**Table 2.** Raw Data from NSF Interactive Earthquake Browser (1990 - 2015)

| Raw Data  |                     |
|-----------|---------------------|
| Features  | Range               |
| Year      | 1990 - 2015         |
| Month     | 1 - 12              |
| Day       | 1- 31               |
| Time      | 00:00:00 - 23:59:59 |
| Latitude  | 33 - 44             |
| Longitude | 17 - 44             |
| Region    | 1 - 28              |
| Depth     | 0.00 - 800.00       |
| Magnitude | 1 - 10              |
| Timestamp |                     |

**Table 3.** Utilized Data from NSF Interactive Earthquake Browser (1990 - 2015)

| Utilized Data           |                     |        |
|-------------------------|---------------------|--------|
| Features                | Range               | Class  |
| Year                    | 1990 - 2015         |        |
| Epoch Code              | 1 - 12              | 0 - 3  |
| Day Code                | 1 - 31              | 0 - 2  |
| Time Code               | 00:00:00 - 23:59:59 | 0 - 3  |
| Latitude                | 33 - 44             |        |
| Longitude               | 17 - 44             |        |
| Depth Code              | 0.00 - 800.00       | 0 - 5  |
| Previous Magnitude Code | 1 - 10              | 1 - 7  |
| Same Region Code        | 1 - 28              | 1 - 28 |
| Lithospheric Code       | 1 - 7               | 1 - 7  |
| Kp Code                 | 0.000 - 9.000       | 0 - 5  |

Time Code, Latitude, Longitude, Depth Code, Previous Magnitude Code, Same Region Code, Lithospheric/Tectonic Plate, Kp Code. This information is outlined in Table 3.

In the processed dataset, categorical classes were introduced to facilitate the analysis. Specifically, the months were initially ordered numerically and subsequently grouped according to the corresponding season. Thus, class 0 represents the winter months, class 1 corresponds to the spring months, class 2 to the summer months, and class 3 to the autumn months. The days comprising each month were divided into three ten-day intervals, with the first interval assigned to class 0, the second interval to class 1, and the final interval to class 2. Accordingly, the hours of the 24 hour day were divided into distinct periods, with the morning zone assigned to class 0, midday to class 1, afternoon to class 2, and night to class 3. For the depth code, earthquakes occurring near the surface (0-32.9 km) were assigned to class 0, those recorded at depths between 33-69.9 km to class 1, events within 70-149.9 km to class 2, those between 150-299.9 km to class 3, earthquakes at depths of 300-499.9 km to class 4, those between 500-799.9 km to class 5, and finally, events occurring at depths greater than 800 km were assigned to class 6. Continuing, earthquakes with magnitudes below 2.9 were assigned to class 1, those with magnitudes between 3.0-3.9 to class 2, magnitudes between 4.0-4.9 to class 3, magnitudes between 5.0-5.9 to class 4, magnitudes between 6.0-6.9 to class 5, magnitudes between 7.0-7.9 to class 6, while events with magnitudes of 8.0 and above were assigned to class 7. With regard to the categorization of the geographical region and the lithospheric plate, each region was assigned a code ranging from 1 to 28. Similarly, a code from 1 to 7 was allocated to the lithospheric plates corresponding to each seismic event. Finally, the Kp code was classified as follows: values ranging from 0.000-4.000 were assigned to class 0, those from 4.100-5.000 to class 1, values

between 5.100–6.000 to class 2, those from 6.100–7.000 to class 3, values between 7.100–8.000 to class 4, and finally, values from 8.100–9.000 were assigned to class 5.

At the following stage of data processing, we elected to focus on earthquakes with a magnitude code of 2 and above, since the inclusion of lower-magnitude events would bias the model toward predicting minor seismic occurrences. Notably, the small-magnitude category (1-2.9 mag) prevailed as the majority class with 407,144 records, creating a significant imbalance in the dataset. By excluding this dominant class, we aimed to achieve a more balanced distribution across magnitudes and to enhance the representational capacity of the model. This approach is consistent with previous studies that have similarly excluded small earthquakes to mitigate bias and improve predictive performance. Wang et al., in 2023, reports in Dataset and Feature Engineering “The seismic catalog used in this study was obtained from the China Earthquake Data Center (CEDC, <http://data.earthquake.cn/>, last accessed on 12 December 2025) and includes earthquake events with a magnitude greater than 3.0 in the Sichuan-Yunnan region from 1970 to 2021” [62]. It is noteworthy that the division into two classes within the field of seismology has previously been employed, as in the study of Zhang et al. (2023), which investigated seismic data by categorizing events into high magnitude ( $M \geq 5.5$ ) and low magnitude ( $M < 5.5$ ) [64]. Following these steps, we proceeded with our experiments, utilizing approximately 10,000 seismic events in order to generate artificial features through Grammatical Evolution.

In summary, the seismic data employed in this study were recorded on the magnitude scale, covering events from 1 to 10. Initially, we excluded small earthquakes, which predominated in number and affected the balance of the dataset. The data source was the EarthScope Consortium, which operates the NSF Geodetic Facility for the Advancement of Geoscience (GAGE) and the NSF Seismological Facility for the Advancement of Geoscience (SAGE). These records were obtained from thousands of stations worldwide, constituting the primary NSF SAGE archive.

### 2.3. Global optimization methods for neural network training

In the current work two well-known global optimization methods were incorporated for neural network training [65,66], the Genetic Algorithm and the Particle Swarm Optimization (PSO) method. The Genetic algorithms is an evolutionary optimization method designed to minimize an objective function defined over a continuous search space. It operates on a population of candidate solutions, each represented as a vector of parameters and this population is evolved through a series of steps, where in each step some process that resemble natural processes are applied to the population. Genetic algorithms have applied on a wide range applications, that include training of neural networks [68,69]. Beyond neural network training, Genetic Algorithms have demonstrated strong performance in physics, biotechnology, and medical physics. In bioinformatics and biotechnology, they are commonly applied to the analysis of biological data, gene selection, and the optimization of complex biological systems [70]. In medical physics and biomedical engineering, GAs have been successfully used for medical image segmentation [71], diagnostic modeling, and the optimization of treatment parameters [72]. They have also been applied to multi-objective problems related to energy efficiency, economic viability, environmental life-cycle assessment [73] and parameter identification in complex multi-physics energy systems [74]. Also, Figure 4 presents the basic steps of a genetic algorithm.

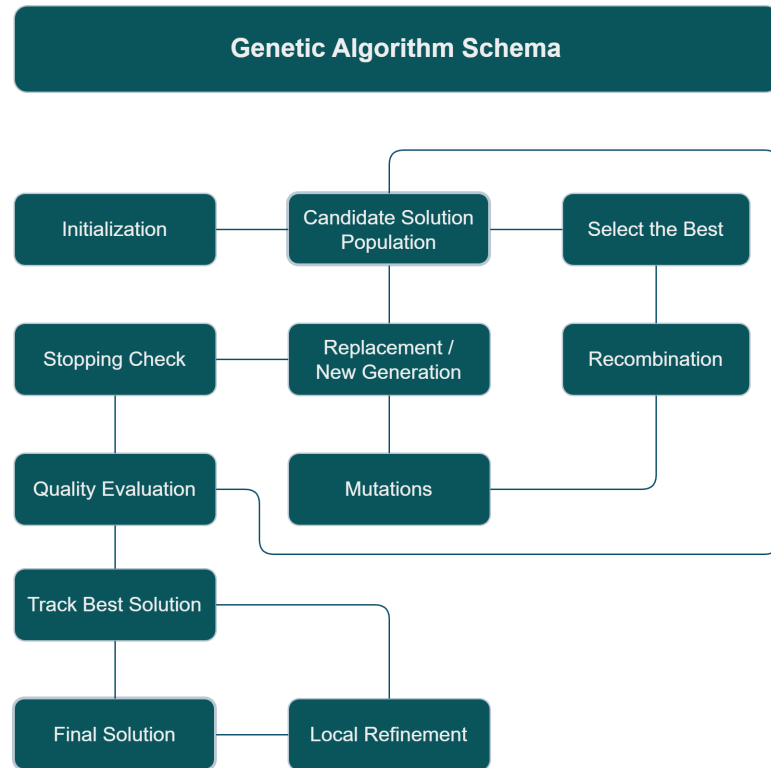


**Figure 4.** The main steps of the Genetic algorithm.

Particle Swarm Optimization (PSO) is a population-based search method inspired by how animals move and cooperate in groups like flocks of birds or schools of fish [76,77]. The PSO was widely used in a variety of practical problems as well as in neural network training [78,79]. Beyond neural network training, Particle Swarm Optimization has been applied across a broad spectrum of scientific and technological domains. In particular, it has found significant use in economic and resource optimization[80], as well as in healthcare management and medical physics, where it supports efficient medical service allocation and the management of stochastic patient queue systems[81]. At the same time, PSO has been increasingly adopted in physics and chemical engineering for the optimization of catalytic processes and energy systems, often in combination with deep learning approaches to extract meaningful physical and chemical insights[82]. In more dynamic and decentralized settings, PSO has proven especially effective in robotics, where it is used to coordinate swarms of autonomous robots during search-and-rescue missions operating under uncertain and rapidly changing conditions[83]. Finally, its flexibility has also led to successful applications in bioinformatics and computational biology, where advanced multi-objective PSO variants are employed for community detection and the identification of disease-related functional modules within complex biological networks[84]. The main steps of the PSO method are outlined in Figure 5.

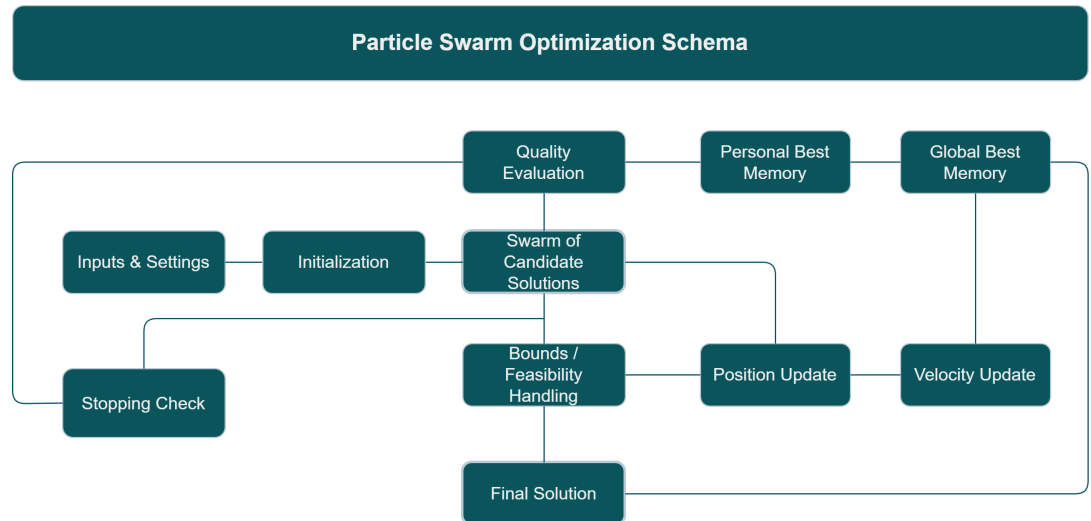


**Figure 5.** The main steps of the PSO algorithm.

#### 2.4. The SVM method

The Support Vector Machine (SVM) is a supervised learning algorithm applied to both classification and regression problems [85]. The concept of Support Vector methods was introduced by V. Vapnik in 1965, in the context of addressing challenges in pattern recognition. During the 1990s, V. Vapnik formally introduced Support Vector Machine (SVM) methods within the framework of Statistical Learning. Since their introduction, SVMs have been extensively employed across diverse domains, including pattern recognition, natural language processing, and related applications [86]. For instance, the SVM algorithm has been employed both in studies on earthquake prediction and in research on the early detection of seismic phenomena, as demonstrated in the following works: Hybrid Technique Using Singular Value Decomposition (SVD) and Support Vector Machine (SVM) Approach for Earthquake Prediction [87], Using Support Vector Machine (SVM) with GPS Ionospheric TEC Estimations to Potentially Predict Earthquake Events [88], The efficacy of support vector machines (SVM) in robust determination of earthquake early warning magnitudes in central Japan [89]. As with other comparative analyses of models, SVMs require greater computational resources during training and exhibit reduced susceptibility to overfitting, whereas neural networks are generally regarded as more adaptable and capable of scaling effectively. Beyond these applications, SVMs have also been widely adopted in several applied scientific and engineering fields. In bioinformatics, SVMs are commonly employed to analyze and interpret complex biological data, where their ability to handle high-dimensional feature spaces is particularly valuable[90]. In medical imaging and clinical applications, they have been used effectively for disease classification and staging, such as the prediction of lung cancer stages from medical imaging data[91]. In addition, SVM-based models are increasingly integrated into healthcare monitoring systems, including Internet of Medical Things (IoMT) frameworks, where reliability and robustness are critical requirements[92]. Moreover, SVMs have been applied in applied physics and engineering, including the prediction of electronic properties in advanced material structures and nanocomposites[93]. Their robustness has also made them suitable for safety-critical applications, such as fault detection and diagnosis in nuclear power plant systems[94].

#### 2.5. The neural network construction method

Another method used in the experiments to predict the category of seismic vibrations is the method of constructing artificial neural networks using Grammatical Evolution [95].

This method can detect the optimal architecture for neural networks as well as the optimal set of values for the corresponding parameters. This method was used in various cases, such as chemistry problems [96], solution of differential equations [97], medical problems [98], educational problems [99], detection of autism [100] etc. This method can produce neural networks in the following form:

$$N(\vec{x}, \vec{w}) = \sum_{i=1}^H w_{(d+2)i-(d+1)} \sigma \left( \sum_{j=1}^d x_j w_{(d+2)i-(d+1)+j} + w_{(d+2)i} \right) \quad (1)$$

In this equation the value  $H$  represents the number of used computation units (weights) for the neural network. The vector  $w$  denotes the vector containing the parameters of the neural network and vector  $x$  represents the input vector (pattern). The function  $\sigma(x)$  stands for the sigmoid function, which is defined as:

$$\sigma(x) = \frac{1}{1 + \exp(-x)} \quad (2)$$

## 2.6. The proposed method

The method proposed here to tackle the classification of seismic events is a procedure that constructs artificial features from the original ones using Grammatical Evolution. The method was initially presented in the paper of Gavrilis et al [101] and used in various cases in the past [102–104]. The main steps of this method have as follows:

### 1. Initialization step.

- (a) Obtain the train data and denote them using the  $M$  pairs  $(x_i, t_i)$ ,  $i = 1..M$ . The values  $t_i$  represent the actual output for the input pattern  $x_i$ .
- (b) Set the parameters of the used genetic algorithm:  $N_g$  for as the number of allowed generations,  $N_c$  for the number of chromosomes,  $p_s$  for the selection rate and  $p_m$  for the mutation rate.
- (c) Set as  $N_f$  the number of artificial features that will construct the current method.
- (d) Initialize every chromosome  $g_i, i = 1, \dots, N_g$  as a set of randomly selected integers.
- (e) Set  $k = 1$ , the generation counter.

### 2. Genetic step

- (a) For  $i = 1, \dots, N_g$  do
  - i. Construct with Grammatical Evolution a set of  $N_f$  artificial features for the each chromosome  $g_i$ . The BNF grammar used for this procedure is shown in Figure 6.
  - ii. Transform the original set of features using the constructed features and denote the new training set as  $(x_{g_i,j}, t_j)$ ,  $j = 1..M$
  - iii. Train a machine learning  $C$  on the new training set. The training error for this model will represent the fitness  $f_i$  for the current chromosome and it is computed as:

$$f_i = \sum_{j=1}^M (C(x_{g_i,j}) - t_j)^2 \quad (3)$$

In the current work the Radial Basis Function networks (RBF) [105,106] were used as the machine learning models. A decisive factor for this

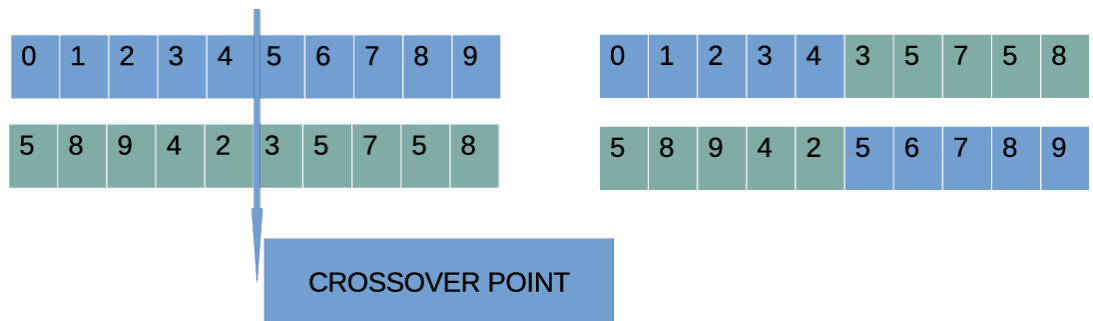
choice was the short training time required for these machine learning models.

- iv. **Perform** the selection procedure: Initially the the chromosomes are sorted according to the associated fitness values and the best  $(1 - p_s) \times N_C$  of them are copied intact to the next generation. The remaining chromosomes will be replaced by offsprings that will be produced during the crossover and the mutation procedure.
- v. **Perform** the crossover procedure: The outcome of this process is a set of  $p_s \times N_c$  new chromosomes. For every pair  $(\tilde{z}, \tilde{w})$  of new chromosomes, two distinct chromosomes  $z$  and  $w$  are chosen from the current population using the process of tournament selection. Afterwards, the new chromosomes are produced using the procedure of one - point crossover, that is illustrated in in Figure 7.
- vi. **Execute** the mutation procedure: during this procedure a random number  $r \in [0, 1]$  is selected for each element of every chromosome. The corresponding element is altered randomly if  $r \leq p_m$ .

(b) **EndFor**

3. **Set**  $k = k + 1$
4. **If**  $k \leq N_g$  goto **Genetic Step**
5. **Obtain the best chromosome**  $g^*$  from the current population.
6. **Create** the corresponding  $N_f$  features for  $g^*$  and apply this features to the set set and report the corresponding test error.

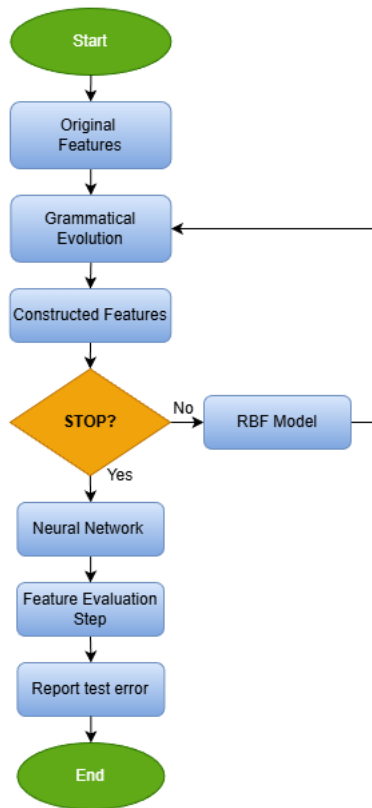
Also, a flowchart that presents the overall process of feature construction is presented in Figure 8.



**Figure 7.** An example of the one - point crossover method.

**Figure 6.** The grammar used for the proposed method.

```
S ::= <expr>      (0)
<expr> ::=  (<expr> <op> <expr>)  (0)
           | <func> ( <expr> )      (1)
           | <terminal>          (2)
<op>  ::=   +     (0)
           | -     (1)
           | *     (2)
           | /     (3)
<func> ::=  sin   (0)
           | cos   (1)
           | exp   (2)
           | log   (3)
<terminal> ::= <xlist>           (0)
               | <digitlist>.<digitlist> (1)
<xlist> ::= x1    (0)
           | x2    (1)
           .....
           | xN    (N)
<digitlist> ::= <digit>        (0)
                | <digit><digit>    (1)
                | <digit><digit><digit> (2)
<digit>  ::=  0 (0)
           | 1 (1)
           | 2 (2)
           | 3 (3)
           | 4 (4)
           | 5 (5)
           | 6 (6)
           | 7 (7)
           | 8 (8)
           | 9 (9)
```

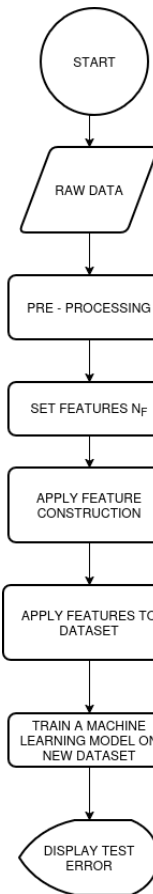


**Figure 8.** The steps of the feature construction procedure.

Moreover, a graphical pipeline that summarizes the whole procedure is depicted in Figure 9.

438

439

**Figure 9.** The pipeline of the used procedure.

### 3. Results

The methods used in the conducted experiments were coded in ANSI C++, with the assistance of the freely available optimization package of OPTIMUS [107]. Moreover, for the feature construction procedure the freely available programming tool QFc, that can be downloaded from <https://github.com/itsoulos/QFc>(accessed on 12 December 2025)[108] has been used. Each experiment was conducted 30 times, using different seed for the random generator in each execution. Also, the procedure of ten - fold cross validation was incorporated to validate the conducted experiments. The values for the experimental parameters are listed in Table 4. The parameters in this table have been chosen to provide a compromise between speed and efficiency of the proposed procedure and were applied to all methods used in the experiments, so that there is fairness in the comparison of experimental results. The proposed method of feature construction was applied to each individual fold and averages of the classification errors in the control sets were obtained. In addition, the RBF machine learning model was used to construct the new features, due to the significantly shorter learning time required for it compared to other models, such as artificial neural networks.

**Table 4.** The values of the experimental parameters.

| PARAMETER | MEANING               | VALUE |
|-----------|-----------------------|-------|
| $N_g$     | Number of generations | 500   |
| $N_c$     | Number of chromosomes | 500   |
| $p_s$     | Selection rate        | 0.9   |
| $p_m$     | Mutation rate         | 0.05  |
| $N_f$     | Number of features    | 2     |

**Table 5.** Experimental results using a series of machine learning methods.

| DATASET        | MLP(GEN)      | MLP(PSO)      | SVM           | NNC           | FC           |
|----------------|---------------|---------------|---------------|---------------|--------------|
| GCT1990        | 39.98%        | 38.21%        | 14.30%        | 22.72%        | 13.50%       |
| GCT1995        | 38.08%        | 33.22%        | 13.48%        | 21.50%        | 10.82%       |
| GCT2000        | 26.70%        | 27.48%        | 10.19%        | 24.59%        | 6.52%        |
| GCT2005        | 38.44%        | 33.19%        | 6.85%         | 27.85%        | 4.45%        |
| GCT2010        | 52.89%        | 44.77%        | 14.46%        | 29.81%        | 9.97%        |
| <b>AVERAGE</b> | <b>39.22%</b> | <b>35.37%</b> | <b>11.86%</b> | <b>25.29%</b> | <b>9.05%</b> |

Table 5 reports the classification error rates for five temporal subsets of the seismic dataset (GCT1990, GCT1995, GCT2000, GCT2005, GCT2010), where the first column encodes the year of the data and the remaining columns correspond to the machine learning models MLP(GEN), MLP(PSO), SVM, NNC, and the proposed FC (Future Constructions) model. The values are expressed as percentage classification error, that is, the proportion of misclassified events between the two seismic classes defined during preprocessing (events with magnitude code 2-3 versus events with magnitude greater than 3). The following notation is used in this table:

1. The column MLP(GEN) denotes the error from the application of the genetic algorithm described in subsection 2.3 for the training of a neural network with 10 processing nodes.
2. The column MLP(PSO) represents the incorporation of the PSO method given in subsection 2.3 for the training of a neural network with 10 processing nodes.
3. The column SVM represent the application of the SVM method, described in subsection 2.4. In the current implementation the freely available library LibSvm [109] was used.
4. The column NNC represents the neural network construction method, described in subsection 2.5.
5. The column FC denotes the proposed feature construction technique, outlined in subsection 2.6.
6. The row AVERAGE denotes the average classification error for all datasets.

Also, Table 6 indicates the precision and recall values for SVM, NNC and the proposed method.

**Table 6.** Precision and recall values for the methods SVM, NNC and FC.

| DATASET | SVM       |        | NNC       |        | FC        |        |
|---------|-----------|--------|-----------|--------|-----------|--------|
|         | PRECISION | RECALL | PRECISION | RECALL | PRECISION | RECALL |
| GCT1990 | 0.798     | 0.837  | 0.684     | 0.728  | 0.800     | 0.874  |
| GCT1995 | 0.811     | 0.830  | 0.684     | 0.729  | 0.801     | 0.886  |
| GCT2000 | 0.835     | 0.844  | 0.662     | 0.700  | 0.835     | 0.901  |
| GCT2005 | 0.856     | 0.869  | 0.628     | 0.627  | 0.856     | 0.904  |
| GCT2010 | 0.802     | 0.824  | 0.633     | 0.628  | 0.804     | 0.805  |

The most striking observation is that FC achieves the lowest error for all five datasets, with no exceptions. For every GCT year, the FC column attains the minimum error among all models, demonstrating a consistent and temporally robust superiority. This pattern is clearly reflected in the AVERAGE row: the mean classification error of FC is 9.05%, whereas the corresponding mean error of the best conventional baseline, the SVM, is 11.86%. Moving from 11.86% to 9.05% corresponds to an error reduction of approximately 24-25%, meaning that roughly one quarter of the misclassifications made by the SVM are eliminated when using FC. Compared with the neural approaches, the gain is even more pronounced: FC reduces the mean error from 39.22% to 9.05% for MLP(GEN), from 35.37% to 9.05% for

MLP(PSO), and from 25.29% to 9.05% for NNC, effectively absorbing about 64-77% of their errors.

Examining the behaviour per year reveals how the proposed model interacts with the specific characteristics of each temporal subset. Dataset GCT2005 appears to be the “easiest” case for all models, with the SVM dropping to 6.85% error and FC reaching 4.45%, which corresponds to an accuracy of about 95.5%. At the opposite end of the spectrum, GCT2010 is clearly the most challenging dataset, as indicated by substantially increased errors for the conventional models (MLP(GEN) 52.89%, MLP(PSO) 44.77%, NNC 29.81%) and by a higher error for the SVM (14.46%). Even in this difficult scenario, FC keeps the error below 10% (9.97%), preserving a clear qualitative advantage in the most demanding temporal setting. A similar pattern emerges for the intermediate years 1995 and 2000, where FC-SVM absolute differences are in the range of 2-4 percentage points, corresponding to roughly 20-35% relative error reduction. This suggests that as the data become more complex, the benefit of the automatically constructed features generated by Grammatical Evolution becomes increasingly pronounced.

A second important finding is that the ranking of the conventional models remains stable across all years. The SVM is consistently the best among the standard baselines, followed by NNC and the two MLP variants, with MLP(PSO) systematically outperforming MLP(GEN). This stability reinforces the credibility of the table as a benchmark, indicating that the results are not driven by noise or random fluctuations but instead reflect a coherent hierarchy of model performance. On top of this stable baseline, FC does not merely swap the winner for a single dataset, it establishes a new performance level by consistently pushing the error rates to substantially lower values in every year.

From a practical standpoint, given that the final processed dataset contains on the order of 10,000 seismic events, an average error of 11.86% compared with 9.05% implies hundreds fewer misclassified instances when FC is used instead of a plain SVM trained on the original features. This has direct implications for early warning and risk assessment applications, where each reduction in misclassification translates into more reliable decision-making. The evidence from Table 5, combined with the methodological description, strongly supports the view that the feature construction phase based on Grammatical Evolution is not a minor refinement over existing classifiers, but rather a key component that reshapes the feature space so that the seismic classes become much more separable. This explains why the proposed FC model achieves an average error of approximately 9%, in full agreement with the reported overall accuracy of 91% in the abstract.

Overall, Table 6 shows that FC is not only the best-performing model in each individual year but also the most stable across different temporal subsets, confirming that the future-construction approach with Grammatical Evolution yields a substantial and consistent improvement over standard machine learning models for the discrimination of seismic events.

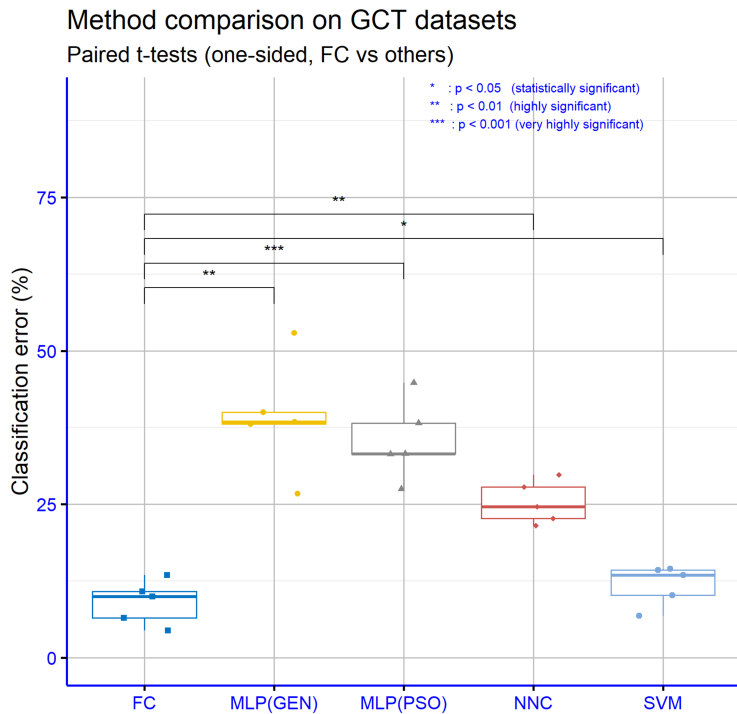


**Figure 10.** Comparison of FC and baseline classifiers on GCT datasets (paired one-sided t-tests on classification error)

The repeated-measures ANOVA with Method as the within-subject factor and DATASET (year) as the blocking factor confirms that the choice of classifier has a statistically significant effect on the classification error, indicating that the models are not equivalent in terms of predictive performance. Building on this global result, we conducted pairwise paired t-tests between the proposed FC model and each baseline, using one-sided alternatives that explicitly test the hypothesis that FC achieves lower mean error than its competitors. The resulting p-values, visualised as significance stars on the boxplot, show that the superiority of FC is statistically supported across all comparisons (Figure 10).

In particular, the comparisons FC vs MLP(GEN) and FC vs NNC yield \*\* ( $p < 0.01$ ), indicating that the probability of observing differences of this magnitude in favour of FC purely by chance is below 1%. An even stronger effect emerges for FC vs MLP(PSO), which is marked with \*\*\* ( $p < 0.001$ ), reflecting the very large performance gap between FC and the PSO-trained MLP. Finally, the comparison FC vs SVM is annotated with \* ( $p < 0.05$ ), showing that, although the numerical difference in error is smaller than in the neural baselines, it remains statistically significant in favour of FC. Overall, the pattern of significance codes (\*, \*\*, \*\*\*) corroborates the message of Table 6: FC is not only the best-performing model in terms of average classification error, but its advantage over all other methods is statistically significant, with particularly strong evidence against the MLP-based models and clear, though more moderate, evidence against the already very competitive SVM baseline.

Also, a graphical summary that represents graphically the comparison between the different machine learning methods is depicted in Figure 11.

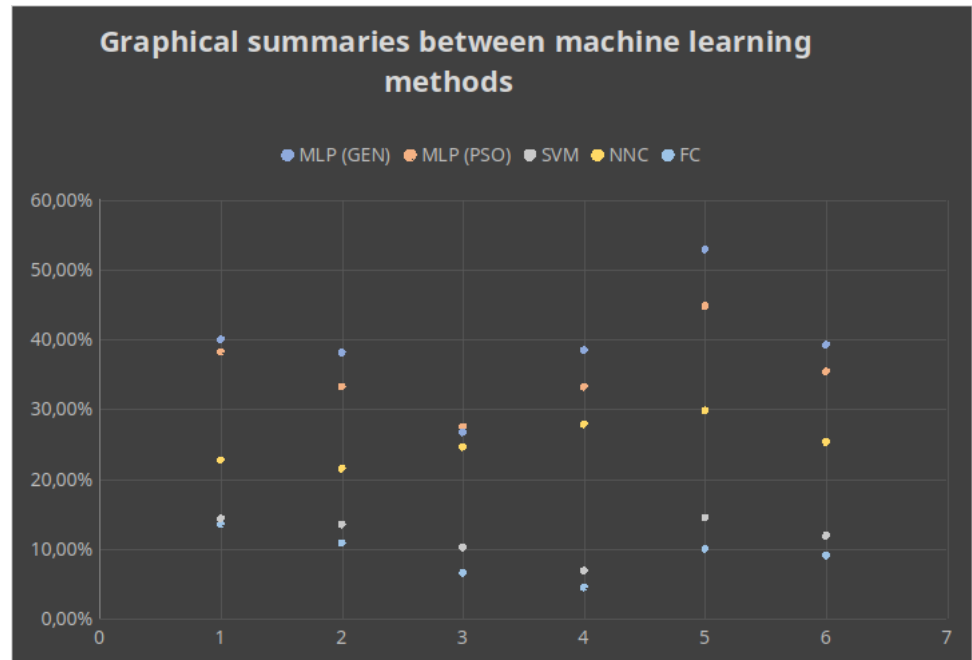


**Figure 11.** Graphical comparison of the used machine learning methods.

Moreover, the proposed method can identify the hidden relationships between the features of the objective dataset. As an example of constructed features consider the following two features created for a distinct run on the GCT2010 dataset:

$$\begin{aligned} f_1(x) &= \sin((28.841/9.28) * x_{10} + (-78.60) * x_3 + 16.12 * x_7 + 6.3 * x_{11}) \\ f_2(x) &= \cos(458.6 * x_2 + (-18.809) * x_4) \end{aligned}$$

The following figures provide a concise visual characterization of the artificial features generated by Grammatical Evolution: (i) expression-tree representations for two representative constructed features ( $f_1, f_2$ ) and (ii) a complementary summary of the grammar primitives used in these constructions, offering direct insight into both their structural form and their basic building blocks.

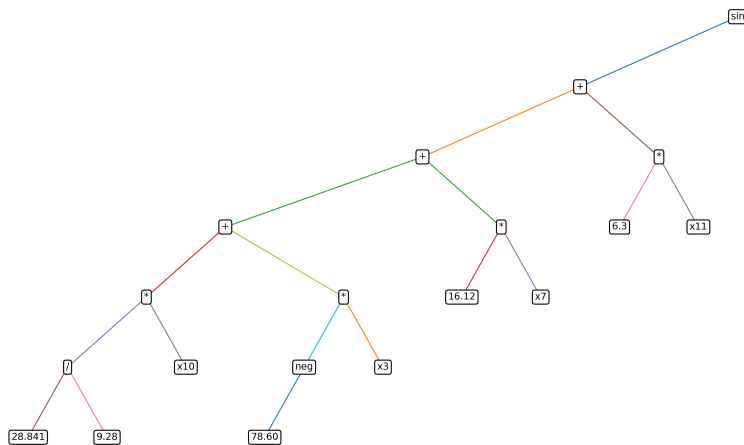


**Figure 12.** Constructed feature  $f_1(x)$  expression tree

Figure 12 (expression tree of  $f_1$ ) visualizes the internal structure of the first constructed feature as an expression tree. The root node corresponds to the non-linear primitive sin, applied to an algebraic core that combines multiple original variables ( $x_{10}, x_3, x_7, x_1$ )

through a weighted sum with constants. This diagram provides an interpretable view of the GE output, indicating that non-linearity is applied over algebraic forms of controlled complexity assembled from grammar primitives.

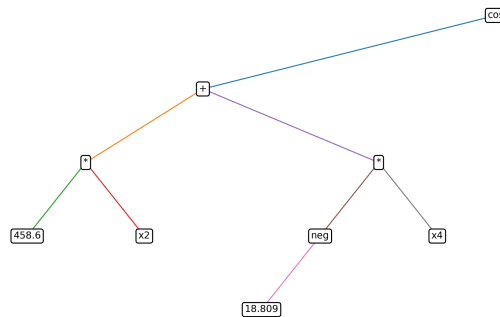


**Figure 13.** Constructed feature  $f_2(x)$  expression tree

Figure 13 (expression tree of  $f_2$ ) depicts a second constructed feature with a simpler topology: a  $\cos$  root applied to the sum of two variable terms ( $x_2, x_4$ ) with constant coefficients. Compared to  $f_1$ , this construction has lower structural complexity (fewer nodes/terms) while still introducing non-linearity. The contrast between the two trees illustrates that GE can produce features of varying complexity, ranging from compact to richer expressions, depending on the optimization objective.

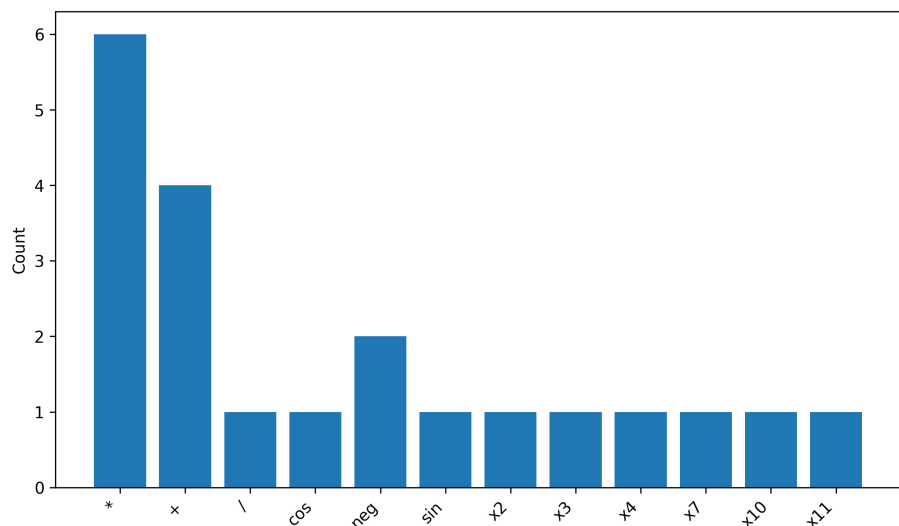


**Figure 14.** Grammar primitives used in example constructed features ( $f_1, f_2$ )

Figure 14 (primitive usage) summarizes the grammar building blocks used in the example constructions ( $f_1, f_2$ ), including non-linear functions ( $\sin/\cos$ ), arithmetic operators ( $+, *, /$ ), and terminal variables  $x_i$ . Bar heights correspond to simple occurrence counts (node counts) of primitives within the two symbolic expressions, while numeric constants are omitted to keep the visualization compact and focused on structural elements. This plot provides an intuitive view of the “vocabulary” employed in these constructions, and the same analysis can be extended by aggregating counts over all runs to describe broader construction trends.

### 3.1. Experiments with the number of features

An additional experiment was conducted, where the number of constructed features was changed from 1 to 4 for the proposed feature construction method. The corresponding experimental results are outlined in Table 7.

**Table 7.** Experimental results using the proposed method and a series of values for the number of constructed features  $N_f$ .

| DATASET | $N_f = 1$ | $N_f = 2$ | $N_f = 3$ | $N_f = 4$ |
|---------|-----------|-----------|-----------|-----------|
| GCT1990 | 11.03%    | 13.50%    | 14.62%    | 15.40%    |
| GCT1995 | 9.41%     | 10.82%    | 9.98%     | 10.05%    |
| GCT2000 | 6.51%     | 6.52%     | 6.75%     | 6.54%     |
| GCT2005 | 4.40%     | 4.45%     | 4.42%     | 4.38%     |
| GCT2010 | 9.72%     | 9.97%     | 9.82%     | 10.32%    |
| AVERAGE | 8.21%     | 9.05%     | 9.12%     | 9.34%     |

Table 7 investigates the behavior of the proposed FC model as the number of constructed features  $N_f$  varies from 1 to 4. The results show that performance is generally very stable, with the mean classification error ranging within a narrow band between 8.21% (for  $N_f = 1$ ) and 9.34% (for  $N_f = 4$ ). The lowest average error is obtained with a single constructed feature ( $N_f = 1$ ), whereas the configuration  $N_f = 2$ , which is adopted as the default setting in Table 5, yields a mean error of 9.05%, very close to the optimum and with highly consistent behaviour across all years. In some datasets, such as GCT2005, slightly better values appear for larger  $N_f$  (e.g., 4.38% for  $N_f = 4$  versus 4.40% for  $N_f = 1$ ), but these gains are marginal and do not change the overall picture. Taken together, the results indicate that FC does not require a large number of future constructions to perform well: one or two constructed features are sufficient to achieve very low error rates, while further increasing  $N_f$  does not lead to systematic improvements and likely introduces redundant information that does not translate into better generalization. This supports the view that the quality of the features generated by Grammatical Evolution is more important than their quantity, and that the proposed choice  $N_f = 2$  offers a well-balanced compromise between performance and model simplicity. Also, Figure 15 presents a comparison for the test error for various cases of the parameter  $N_f$ .

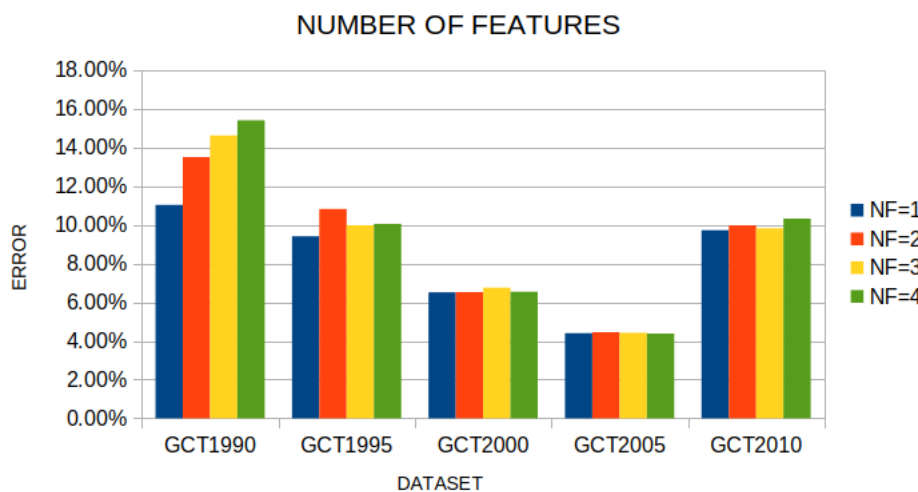


**Figure 15.** The performance of the proposed method on the used datasets, using various values for the parameter  $N_f$ .

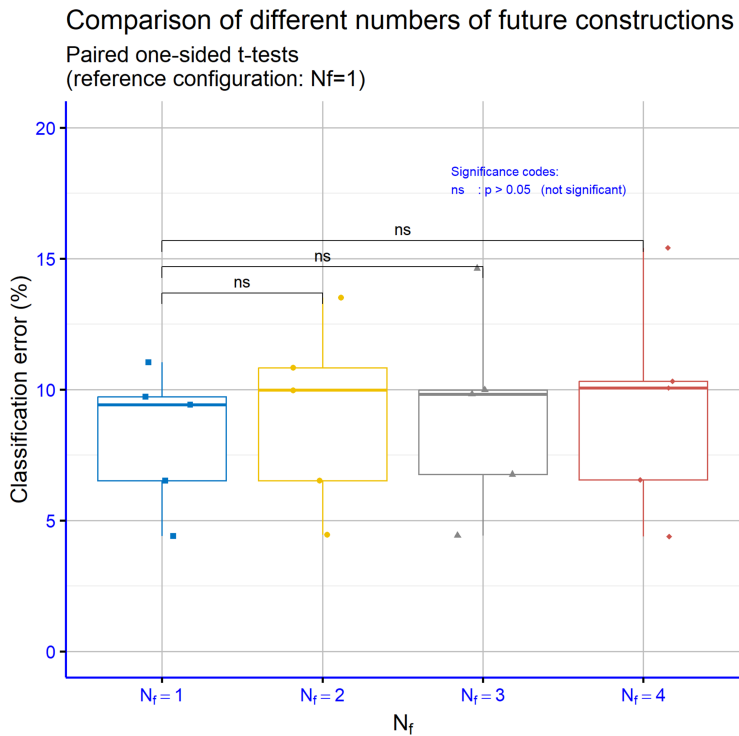


**Figure 16.** Comparison of FC and baseline classifiers on GCT datasets (paired one-sided t-tests on classification error)

The boxplot for Table 7, together with the paired t-tests, shows that none of the comparisons among the  $N_f = 1$ ,  $N_f = 2$ ,  $N_f = 3$  and  $N_f = 4$  configurations reaches statistical significance (all labelled as ns). This indicates that, given the available datasets, the performance of the FC model is essentially insensitive to the number of future constructions, and that using smaller values such as  $N_f = 1$  or  $N_f = 2$  achieves comparable accuracy without any statistically supported gains from increasing  $N_f$  (Figure 16).

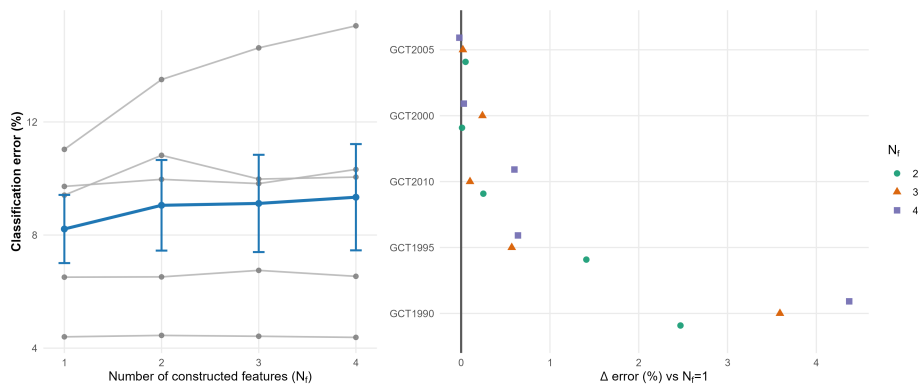


**Figure 17.** Effect of the number of constructed features  $N_f$ : consistency of  $N_f=1$  and diminishing returns

The Figure 17 summarizes how the classification error varies with the number of constructed features  $N_f$ . The left panel plots error versus  $N_f$  for each dataset, together with the mean trend ( $\pm$  standard error), indicating that the lowest average error is obtained at  $N_f=1$ . The right panel reports the per-dataset difference  $\Delta = \text{Error}(N_f=k) - \text{Error}(N_f=1)$  for  $k \geq 2$ , where the dashed line  $\Delta=0$  corresponds to the  $N_f=1$  baseline. Predominantly positive  $\Delta$  values show that increasing  $N_f$  provides no additional benefit and leads to diminishing returns relative to  $N_f=1$ .

### 3.2. Experiments with the number of generations

Moreover, in order to test the efficiency of the proposed method, an additional experiment was executed, where the number of generations was altered from 50 to 400.

**Table 8.** Experimental results using the proposed method and a series of values for the number of generations  $N_g$ .

| DATASET        | $N_g = 50$   | $N_g = 100$  | $N_g = 200$  | $N_g = 400$  |
|----------------|--------------|--------------|--------------|--------------|
| GCT1990        | 13.61%       | 13.19%       | 13.50%       | 12.30%       |
| GCT1995        | 11.06%       | 11.70%       | 10.82%       | 10.74%       |
| GCT2000        | 6.53%        | 6.58%        | 6.52%        | 6.52%        |
| GCT2005        | 4.58%        | 4.45%        | 4.45%        | 4.41%        |
| GCT2010        | 9.88%        | 10.00%       | 9.97%        | 9.94%        |
| <b>AVERAGE</b> | <b>9.13%</b> | <b>9.18%</b> | <b>9.05%</b> | <b>8.78%</b> |

Table 8 focuses on the number of generations  $N_g$  of the evolutionary algorithm during feature construction and evaluates four values (50, 100, 200, 400). The results demonstrate that FC is remarkably robust with respect to this hyperparameter: the mean classification error remains very close across settings, ranging from 9.18% for  $N_g = 100$  down to 8.78% for  $N_g = 400$ . The configuration  $N_g = 200$ , which is used as the default in the previous analysis, attains an average error of 9.05%, essentially indistinguishable from the more expensive setting  $N_g = 400$ , which improves the mean error only by about a quarter of a percentage point. At the level of individual datasets there are cases where a larger number of generations yields more noticeable gains (for instance, GCT1990 improves to 12.30% at  $N_g = 400$ ), but the overall pattern is that most of the benefit is already captured within 100-200 generations, with further iterations providing diminishing returns. Thus, Table 8 suggests that the Grammatical Evolution process converges to useful future constructions relatively quickly, and that the choice  $N_g = 200$  offers a very good trade-off between computational cost and predictive performance, avoiding unnecessary increases in training time without delivering substantial accuracy gains. Furthermore, Figure 18 outlines the performance of the proposed method for the used datasets, using different values for the number of generations  $N_g$ .

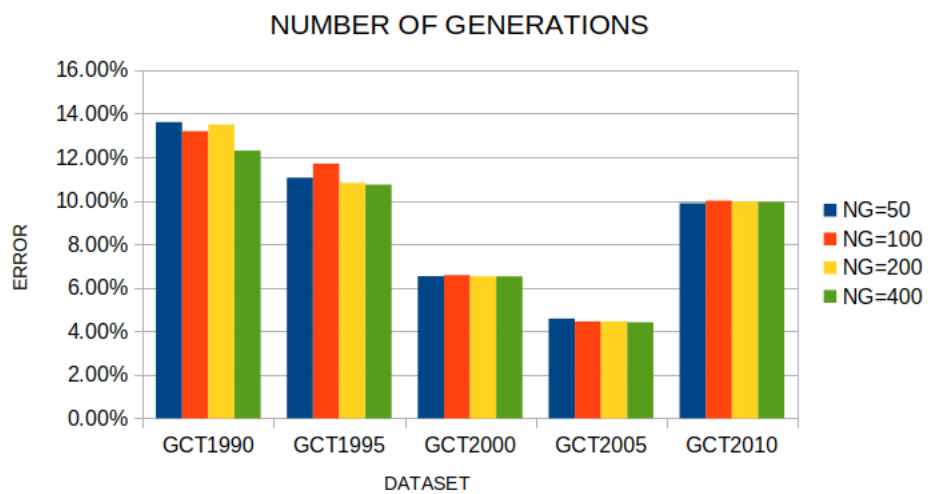


**Figure 18.** The performance of the proposed method using different values for the parameter  $N_g$ .

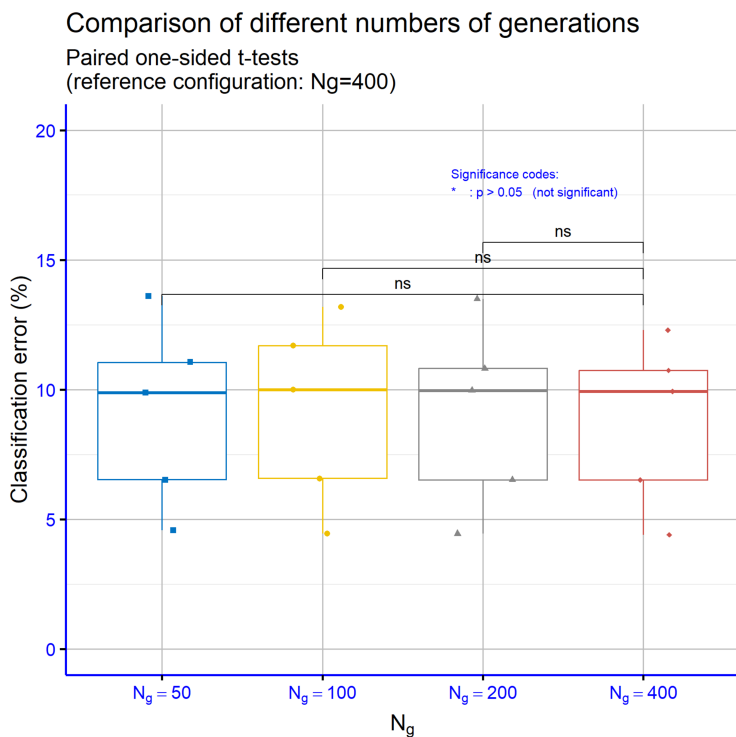


**Figure 19.** Comparison of FC and baseline classifiers on GCT datasets (paired one-sided t-tests on classification error)

In Figure 19, the paired t-tests for the different numbers of generations show that all pairwise comparisons are non-significant (ns), indicating that variations in  $N_g$  do not materially affect the classification error of the FC model.

#### 4. Conclusions

This study investigates the use of Grammatical Evolution for constructing artificial features in earthquake prediction, applying several machine learning approaches, including MLP(GEN), MLP(PSO), SVM, and NNC, alongside Feature Construction (FC). The analysis is based on seismic data recorded between 1990 and 2015 within the geographical area defined by latitudes  $33^{\circ}$ - $44^{\circ}$  and longitudes  $17^{\circ}$ - $44^{\circ}$ . While all the aforementioned methods belong to the domain of machine learning, FC is distinguished as a feature engineering technique. Specifically, Feature Construction (FC) refers to the process of generating new, informative attributes from the existing dataset, thereby enhancing the representational capacity of the data and improving the performance of machine learning models. Following these steps, our experiments demonstrated that the FC technique yielded the best results, achieving the lowest mean error 9.05% corresponding to an overall accuracy of 91%. The SVM method achieved the second-best performance, with an average error of 11.86%. Consequently, we proceeded with the FC technique, which yielded the best results, and implemented artificially constructed features  $N_f$  with ranging from 1 to 4. Furthermore, to evaluate the efficiency of the proposed method, an additional experiment was conducted in which the number of generations  $N_g$  was varied from 50 to 400. Consequently, we applied 1, 2, 3, and 4 constructed features within this technique, with the single constructed feature  $N_f = 1$  exhibiting superior performance compared to the others producing the minimal average error 8.21%. Our experiment was further extended by incorporating a series of values for the number of generations  $N_g$  (50, 100, 200, and 400), and the results indicated that  $N_g = 400$  generations yielded the best performance 8.78%. In contrast, selecting  $N_g = 200$  provides also an effective balance between computational cost and predictive performance. This study

was conducted as a direct response to the challenge identified in our previous research, thereby extending and refining the scope of the earlier findings.

Specifically, the study demonstrates the potential of Grammatical Evolution as a novel feature engineering tool in seismology, offering a new perspective on how artificial features can enhance earthquake prediction models. At the same time, certain limitations must be acknowledged, such as the imbalance in the dataset and the restriction to a specific geographical region, which may affect generalizability. Future research should therefore explore the application of this approach to diverse seismic catalogs, investigate its integration with machines learning architectures. By articulating these implications, limitations, and directions, the contribution of the study becomes clearer and more impactful.

**Author Contributions:** Conceptualization, C.K. and I.G.T.; methodology, C.K.; software, I.G.T.; validation, G.K. C.S., V.C.; formal analysis, G.K.; investigation, C.K.; resources, C.S.; data curation, C.K.; writing original draft preparation, C.K.; writing review and editing, I.G.T.; visualization, V.C.; supervision, C.S.; project administration, C.S.; funding acquisition, C.S. All authors have read and agreed to the published version of the manuscript.

**Funding:** This research has been financed by the European Union : Next Generation EU through the Program Greece 2.0 National Recovery and Resilience Plan , under the call RESEARCH-CREATE-INNOVATE, project name “iCREW: Intelligent small craft simulator for advanced crew training using Virtual Reality techniques” (project code:TAEDK-06195).

**Institutional Review Board Statement:** Not applicable.

**Informed Consent Statement:** Not applicable.

**Data Availability Statement:** The original contributions presented in this study are included in the article. Further inquiries can be directed to the corresponding author.

**Conflicts of Interest:** The authors declare no conflicts of interest.

## References

1. United Nations Office for Disaster Risk Reduction (UNDRR). (2017). Sendai framework terminology on disaster risk reduction. Resilience.
2. Nakamura, Y. (1984). Development of earthquake early-warning system for the Shinkansen, some recent earthquake engineering research and practice in Japan. Proceeding of The Japanese National Committee of the International Association for Earthquake Engineering, June 1984, 224–238.
3. Nakamura, Y. (1988). On the urgent earthquake detection and alarm system (UrEDAS). In Proc. 9th World Conference on Earthquake Engineering, 1988 (pp. 673-678).
4. Espinosa Aranda, J. M., Jimenez, A., Ibarrola, G., Alcantar, F., Aguilar, A., Inostroza, M., & Maldonado, S. (1995). Mexico City seismic alert system. Seismological Research Letters, 66, 42–53
5. Kamigaichi, O., Saito, M., Doi, K., Matsumori, T., Tsukada, S. Y., Takeda, K., ... & Watanabe, Y. (2009). Earthquake early warning in Japan: Warning the general public and future prospects. Seismological Research Letters, 80(5), 717-726.
6. Earthquake Early Warning System (Japan). Wikipedia. Retrieved November 14, 2025, from [https://en.wikipedia.org/wiki/Earthquake\\_Early\\_Warning\\_\(Japan\)](https://en.wikipedia.org/wiki/Earthquake_Early_Warning_(Japan))
7. Wenzel, F., Oncescu, M. C., Baur, M., Fiedrich, F., & Ionescu, C. (1999). An early warning system for Bucharest. Seismological Research Letters, 70(2), 161-169.
8. Alcik, H., Ozel, O., Apaydin, N., & Erdik, M. (2009). A study on warning algorithms for Istanbul earthquake early warning system. Geophysical Research Letters, 36(5).
9. Satriano, C., Elia, L., Martino, C., Lancieri, M., Zollo, A., & Iannaccone, G. (2009, December). The Earthquake Early Warning System for Southern Italy: Concepts, Capabilities and Future Perspectives. In AGU Fall Meeting Abstracts (Vol. 2009, pp. S13A-1726).
10. ShakeAlert. US Geological Survey, Earthquake Hazards Program. Retrieved November 15, 2025, from <https://earthquake.usgs.gov/data/shakealert/>
11. ShakeAlert. Earthquake Early Warning (EEW) System. Retrieved November 15, 2025, from <https://www.shakealert.org/>

12. Zollo, A., Festa, G., Emolo, A., & Colombelli, S. (2015). Source characterization for earthquake early warning. In Encyclopedia of Earthquake Engineering (pp. 3327-3346). Springer, Berlin, Heidelberg. 705
13. Kopitsa, C., Tsoulos, I. G., & Charilogis, V. (2025). Predicting the Magnitude of Earthquakes Using Grammatical Evolution. Algorithms, 18(7), 405. 707
14. Earthquake app. Retrieved November 16, 2025, from [https://earthquake.app/#banner\\_1](https://earthquake.app/#banner_1). 709
15. Android Earthquake Alert System. Retrieved November 16, 2025, from <https://crisisresponse.google/android-early-earthquake-warnings>. 710
16. Greece Earthquakes. Retrieved November 16, 2025, from <https://play.google.com/store/apps/details?id=com.greek.Earthquake&pli=1>. 711
17. Earthquake Network. Retrieved November 16, 2025, from <https://sismo.app/>. 714
18. Housner, G. W., & Jennings, P. C. (1964). Generation of artificial earthquakes. Journal of the Engineering Mechanics Division, 90(1), 113-150. 715
19. Adeli, H., & Panakkat, A. (2009). A probabilistic neural network for earthquake magnitude prediction. Neural networks, 22(7), 1018-1024. 717
20. Zhou, Q., Tong, G., Xie, D., Li, B., & Yuan, X. (2012). A seismic-based feature extraction algorithm for robust ground target classification. IEEE Signal Processing Letters, 19(10), 639-642. 719
21. Martínez-Álvarez, F., Reyes, J., Morales-Esteban, A., & Rubio-Escudero, C. (2013). Determining the best set of seismicity indicators to predict earthquakes. Two case studies: Chile and the Iberian Peninsula. Knowledge-Based Systems, 50, 198-210. 721
22. Schmidt, L., Hegde, C., Indyk, P., Lu, L., Chi, X., & Hohl, D. (2015, April). Seismic feature extraction using Steiner tree methods. In 2015 IEEE international conference on acoustics, speech and signal processing (ICASSP) (pp. 1647-1651). IEEE. 723
23. Narayananakumar, S., & Raja, K. (2016). A BP artificial neural network model for earthquake magnitude prediction in Himalayas, India. Circuits and Systems, 7(11), 3456-3468. 725
24. Asencio-Cortés, G., Martínez-Álvarez, F., Morales-Esteban, A., & Reyes, J. (2016). A sensitivity study of seismicity indicators in supervised learning to improve earthquake prediction. Knowledge-Based Systems, 101, 15-30. 727
25. Asim, K. M., Idris, A., Iqbal, T., & Martínez-Álvarez, F. (2018). Earthquake prediction model using support vector regressor and hybrid neural networks. PloS one, 13(7), e0199004. 729
26. Chamberlain, C. J., & Townend, J. (2018). Detecting real earthquakes using artificial earthquakes: On the use of synthetic waveforms in matched-filter earthquake detection. Geophysical Research Letters, 45(21), 11-641. 731
27. Okada, A., & Kaneda, Y. (2018, May). Neural network learning: Crustal state estimation method from time-series data. In 2018 International Conference on Control, Artificial Intelligence, Robotics & Optimization (ICCAIRO) (pp. 141-146). IEEE. 733
28. Lin, J. W., Chao, C. T., & Chiou, J. S. (2018). Determining neuronal number in each hidden layer using earthquake catalogues as training data in training an embedded back propagation neural network for predicting earthquake magnitude. Ieee Access, 6, 52582-52597. 735
29. Zhang, L., Si, L., Yang, H., Hu, Y., & Qiu, J. (2019). Precursory pattern based feature extraction techniques for earthquake prediction. IEEE Access, 7, 30991-31001. 738
30. Rojas, O., Otero, B., Alvarado, L., Mus, S., & Tous, R. (2019). Artificial neural networks as emerging tools for earthquake detection. Computación y Sistemas, 23(2), 335-350. 740
31. Ali, A., Sheng-Chang, C., & Shah, M. (2020). Continuous wavelet transformation of seismic data for feature extraction. SN Applied Sciences, 2(11), 1835. 742
32. Bamer, F., Thaler, D., Stoffel, M., & Markert, B. (2021). A monte carlo simulation approach in non-linear structural dynamics using convolutional neural networks. Frontiers in Built Environment, 7, 679488. 744
33. Wang, T., Bian, Y., Zhang, Y., & Hou, X. (2023). Using artificial intelligence methods to classify different seismic events. Seismological Society of America, 94(1), 1-16. 746
34. Ozkaya, S. G., Baygin, M., Barua, P. D., Tuncer, T., Dogan, S., Chakraborty, S., & Acharya, U. R. (2024). An automated earthquake classification model based on a new butterfly pattern using seismic signals. Expert Systems with Applications, 238, 122079. 748
35. Sinha, D. K., & Kulkarni, S. (2025, June). Advancing Seismic Prediction through Machine Learning: A Comprehensive Review of the Transformative Impact of Feature Engineering. In 2025 International Conference on Emerging Trends in Industry 4.0 Technologies (ICETI4T) (pp. 1-8). IEEE. 750
36. Mahmoud, A., Alrusaini, O., Shafie, E., Aboalndr, A., & Elbelkasy, M. S. (2025). Machine Learning-Based Earthquake Prediction: Feature Engineering and Model Performance Using Synthetic Seismic Data. Appl. Math, 19(3), 695-702. 753
37. O'Neill, M., & Ryan, C. (2002). Grammatical evolution. IEEE Transactions on Evolutionary Computation, 5(4), 349-358. 755
38. Kramer, O. (2017). Genetic algorithms. In Genetic algorithm essentials (pp. 11-19). Cham: Springer International Publishing. 756
39. Backus, J. W. (1959). The syntax and the semantics of the proposed international algebraic language of the Zurich ACM-GAMM Conference. In ICIP Proceedings (pp. 125-132). 757

40. Ryan, C., Collins, J. J., & Neill, M. O. (1998, April). Grammatical evolution: Evolving programs for an arbitrary language. In European conference on genetic programming (pp. 83-96). Berlin, Heidelberg: Springer Berlin Heidelberg. 759
41. O'Neill, M., & Ryan, C. (1999, May). Evolving multi-line compilable C programs. In European Conference on Genetic Programming (pp. 83-92). Berlin, Heidelberg: Springer Berlin Heidelberg. 760
42. Brabazon, A., & O'Neill, M. (2006). Credit classification using grammatical evolution. *Informatica*, 30(3). 761
43. Şen, S., & Clark, J. A. (2009, March). A grammatical evolution approach to intrusion detection on mobile ad hoc networks. In Proceedings of the second ACM conference on Wireless network security (pp. 95-102). 762
44. Chen, L., Tan, C. H., Kao, S. J., & Wang, T. S. (2008). Improvement of remote monitoring on water quality in a subtropical reservoir by incorporating grammatical evolution with parallel genetic algorithms into satellite imagery. *Water Research*, 42(1-2), 296-306. 763
45. Hidalgo, J. I., Colmenar, J. M., Risco-Martin, J. L., Cuesta-Infante, A., Maqueda, E., Botella, M., & Rubio, J. A. (2014). Modeling glycemia in humans by means of grammatical evolution. *Applied Soft Computing*, 20, 40-53. 764
46. Tavares, J., & Pereira, F. B. (2012, April). Automatic design of ant algorithms with grammatical evolution. In European conference on genetic programming (pp. 206-217). Berlin, Heidelberg: Springer Berlin Heidelberg. 765
47. Zapater, M., Risco-Martín, J. L., Arroba, P., Ayala, J. L., Moya, J. M., & Hermida, R. (2016). Runtime data center temperature prediction using grammatical evolution techniques. *Applied Soft Computing*, 49, 94-107. 766
48. Ryan, C., O'Neill, M., & Collins, J. J. (1998, June). Grammatical evolution: Solving trigonometric identities. In proceedings of Mendel (Vol. 98, p. 4th). Brno, Czech Republic: Technical University of Brno, Faculty of Mechanical Engineering. 767
49. de la Puente, A. O., Alfonso, R. S., & Moreno, M. A. (2002, June). Automatic composition of music by means of grammatical evolution. In Proceedings of the 2002 conference on APL: array processing languages: lore, problems, and applications (pp. 148-155). 768
50. De Campos, L. M. L., de Oliveira, R. C. L., & Roisenberg, M. (2016). Optimization of neural networks through grammatical evolution and a genetic algorithm. *Expert Systems with Applications*, 56, 368-384. 769
51. Soltanian, K., Ebnesasir, A., & Afsharchi, M. (2022). Modular grammatical evolution for the generation of artificial neural networks. *Evolutionary computation*, 30(2), 291-327. 770
52. Dempsey, I., O'Neill, M., & Brabazon, A. (2007). Constant creation in grammatical evolution. *International Journal of Innovative Computing and Applications*, 1(1), 23-38. 771
53. Galván-López, E., Swafford, J. M., O'Neill, M., & Brabazon, A. (2010, April). Evolving a ms. pacman controller using grammatical evolution. In European Conference on the Applications of Evolutionary Computation (pp. 161-170). Berlin, Heidelberg: Springer Berlin Heidelberg. 772
54. Shaker, N., Nicolau, M., Yannakakis, G. N., Togelius, J., & O'Neill, M. (2012, September). Evolving levels for super mario bros using grammatical evolution. In 2012 IEEE Conference on Computational Intelligence and Games (CIG) (pp. 304-311). IEEE. 773
55. Martínez-Rodríguez, D., Colmenar, J. M., Hidalgo, J. I., Villanueva Micó, R. J., & Salcedo-Sanz, S. (2020). Particle swarm grammatical evolution for energy demand estimation. *Energy Science & Engineering*, 8(4), 1068-1079. 774
56. Sabar, N. R., Ayob, M., Kendall, G., & Qu, R. (2013). Grammatical evolution hyper-heuristic for combinatorial optimization problems. *IEEE Transactions on Evolutionary Computation*, 17(6), 840-861. 775
57. Ryan, C., Kshirsagar, M., Vaidya, G., Cunningham, A., & Sivaraman, R. (2022). Design of a cryptographically secure pseudo random number generator with grammatical evolution. *Scientific reports*, 12(1), 8602. 776
58. Pereira, P. J., Cortez, P., & Mendes, R. (2021). Multi-objective grammatical evolution of decision trees for mobile marketing user conversion prediction. *Expert Systems with Applications*, 168, 114287. 777
59. Castejón, F., & Carmona, E. J. (2018). Automatic design of analog electronic circuits using grammatical evolution. *Applied Soft Computing*, 62, 1003-1018. 778
60. Tsoulos, I. G., Tzallas, A., & Karvounis, E. (2023). Constructing the Bounds for Neural Network Training Using Grammatical Evolution. *Computers*, 12(11), 226. 779
61. Tsoulos, I. G., Varvaras, I., & Charilogis, V. (2024). RbfCon: Construct Radial Basis Function Neural Networks with Grammatical Evolution. *Software* (2674-113X), 3(4). 780
62. Wang, X., Zhong, Z., Yao, Y., Li, Z., Zhou, S., Jiang, C., & Jia, K. (2023). Small Earthquakes Can Help Predict Large Earthquakes: A Machine Learning Perspective. *Applied Sciences*, 13(11), 6424. 781
63. Gutenberg, B., & Richter, C. F. (1955). Magnitude and energy of earthquakes. *Nature*, 176(4486), 795-795. 782
64. Zhu, J., Zhou, Y., Liu, H., Jiao, C., Li, S., Fan, T., ... & Song, J. (2023). Rapid earthquake magnitude classification using single station data based on the machine learning. *IEEE Geoscience and Remote Sensing Letters*, 21, 1-5. 783
65. Abiodun, O. I., Jantan, A., Omolara, A. E., Dada, K. V., Mohamed, N. A., & Arshad, H. (2018). State-of-the-art in artificial neural network applications: A survey. *Heliyon*, 4(11). 784
66. Suryadevara, S., & Yanamala, A. K. Y. (2021). A Comprehensive Overview of Artificial Neural Networks: Evolution, Architectures, and Applications. *Revista de Inteligencia Artificial en Medicina*, 12(1), 51-76. 785

67. Sivanandam, S. N., & Deepa, S. N. (2008). Genetic algorithms. In *Introduction to genetic algorithms* (pp. 15-37). Berlin, Heidelberg: Springer Berlin Heidelberg. 813
68. Kalogirou, S. A. (2004). Optimization of solar systems using artificial neural-networks and genetic algorithms. *Applied Energy*, 77(4), 383-405. 815
69. Chiroma, H., Noor, A. S. M., Abdulkareem, S., Abubakar, A. I., Hermawan, A., Qin, H., ... & Herawan, T. (2017). Neural networks optimization through genetic algorithm searches: a review. *Appl. Math. Inf. Sci.*, 11(6), 1543-1564. 817
70. Manning, T., Sleator, R. D., & Walsh, P. (2013). Naturally selecting solutions: the use of genetic algorithms in bioinformatics. *Bioengineered*, 4(5), 266-278. 819
71. Maulik, U. (2009). Medical image segmentation using genetic algorithms. *IEEE Transactions on information technology in biomedicine*, 13(2), 166-173. 821
72. Ghaheri, A., Shoar, S., Naderan, M., & Hoseini, S. S. (2015). The applications of genetic algorithms in medicine. *Oman medical journal*, 30(6), 406. 823
73. Mousavi-Avval, S. H., Rafiee, S., Sharifi, M., Hosseinpour, S., Notarnicola, B., Tassielli, G., & Renzulli, P. A. (2017). Application of multi-objective genetic algorithms for optimization of energy, economics and environmental life cycle assessment in oilseed production. *Journal of Cleaner Production*, 140, 804-815. 825
74. Zhang, W., Xie, Y., He, H., Long, Z., Zhuang, L., & Zhou, J. (2025). Multi-physics coupling model parameter identification of lithium-ion battery based on data driven method and genetic algorithm. *Energy*, 314, 134120. 828
75. Kramer, O. (2017). Genetic algorithms. In *Genetic algorithm essentials* (pp. 11-19). Cham: Springer International Publishing. 830
76. Wang, D., Tan, D., & Liu, L. (2018). Particle swarm optimization algorithm: an overview. *Soft computing*, 22(2), 387-408. 831
77. Jain, N. K., Nangia, U., & Jain, J. (2018). A review of particle swarm optimization. *Journal of The Institution of Engineers (India): Series B*, 99(4), 407-411. 832
78. Meissner, M., Schmuker, M., & Schneider, G. (2006). Optimized Particle Swarm Optimization (OPSO) and its application to artificial neural network training. *BMC bioinformatics*, 7(1), 125. 834
79. Garro, B. A., & Vázquez, R. A. (2015). Designing artificial neural networks using particle swarm optimization algorithms. *Computational intelligence and neuroscience*, 2015(1), 369298. 836
80. Li, S. (2025). Economic optimization of business administration resources: Multi-objective scheduling method based on improved PSO. *Journal of Computational Methods in Sciences and Engineering*, 14727978251337955. 838
81. Wang, C. H., Tian, R., Hu, K., Chen, Y. T., & Ku, T. H. (2025). A Markov decision optimization of medical service resources for two-class patient queues in emergency departments via particle swarm optimization algorithm. *Scientific Reports*, 15(1), 2942. 840
82. Bao, R., Wang, Z., Guo, Q., Wu, X., & Yang, Q. (2025). Bio-Digital Catalyst Design: Generative Deep Learning for Multi-Objective Optimization and Chemical Insights in CO<sub>2</sub> Methanation. *ACS Catalysis*, 15(15), 12691-12714. 842
83. Kumar, T. R., Nandhini, T. J., Jumaniyazova, I., Abdulla, H., Jumaniyozov, Y., & Bhatt, V. (2025, May). Swarm Robotics for Search and Rescue Operations in Disaster Zones Using Particle Swarm Optimization (PSO) Algorithms. In *2025 International Conference on Networks and Cryptology (NETCRYPT)* (pp. 870-875). IEEE. 844
84. Zhu, X., Bi, M., Shang, J., Sun, Y., Li, F., Zhang, Y., ... & Liu, J. X. (2025). MPSO-CD: a Multi-objective Particle Swarm Optimization Community Detection Method for Identifying Disease Modules. *IEEE Transactions on Computational Biology and Bioinformatics*. 847
85. Suthaharan, S. (2016). Support vector machine. In *Machine learning models and algorithms for big data classification: thinking with examples for effective learning* (pp. 207-235). Boston, MA: Springer US. 848
86. Wang, Q. (2022, June). Support vector machine algorithm in machine learning. In *2022 IEEE international conference on artificial intelligence and computer applications (ICAICA)* (pp. 750-756). IEEE. 850
87. Astuti, W., Akmelawati, R., Sediono, W., & Salami, M. J. E. (2014). Hybrid technique using singular value decomposition (SVD) and support vector machine (SVM) approach for earthquake prediction. *IEEE Journal of Selected Topics in Applied Earth Observations and Remote Sensing*, 7(5), 1719-1728. 852
88. Asaly, S., Gottlieb, L. A., Inbar, N., & Reuveni, Y. (2022). Using support vector machine (SVM) with GPS ionospheric TEC estimations to potentially predict earthquake events. *Remote Sensing*, 14(12), 2822. 856
89. Reddy, R., & Nair, R. R. (2013). The efficacy of support vector machines (SVM) in robust determination of earthquake early warning magnitudes in central Japan. *Journal of Earth System Science*, 122(5), 1423-1434. 858
90. Mahata, K., Sengupta, S., Biswas, M., Ghosh, S., Banerjee, A. K., Pati, S. K., & Mal, C. (2025). Application of Machine Learning in Bioinformatics: Capture and Interpret Biological Data. In *Machine Learning in Biomedical and Health Informatics* (pp. 239-262). Apple Academic Press. 860
91. Manimaran, P., Vignesh, R., Vignesh, B., & Thilak, G. (2025, February). Enhanced Prediction of Lung Cancer Stages using SVM and Medical Imaging. In *2025 International Conference on Electronics and Renewable Systems (ICEARS)* (pp. 1334-1338). IEEE. 863
92. Kazi, K. S. L. (2025). Machine learning-driven internet of medical things (ML-IoMT)-based healthcare monitoring system. In *Responsible AI for digital health and medical analytics* (pp. 49-86). IGI Global Scientific Publishing. 865

93. Azizian-Kalandaragh, Y., Barkhordari, A., & Badali, Y. (2025). Support vector machine for prediction of the electronic factors of a Schottky configuration interlaid with pure PVC and doped by Sm<sub>2</sub>O<sub>3</sub> nanoparticles. *Advanced Electronic Materials*, 11(6), 2400624. 867  
868  
869
94. Sun, Y., Song, M., Song, C., Zhao, M., & Yang, Y. (2025). KPCA-based fault detection and diagnosis model for the chemical and volume control system in nuclear power plants. *Annals of Nuclear Energy*, 211, 110973. 870  
871  
872
95. Tsoulos, I., Gavrilis, D., & Glavas, E. (2008). Neural network construction and training using grammatical evolution. *Neurocomputing*, 72(1-3), 269-277. 873  
874  
875
96. Papamokos, G. V., Tsoulos, I. G., Demetropoulos, I. N., & Glavas, E. (2009). Location of amide I mode of vibration in computed data utilizing constructed neural networks. *Expert Systems with Applications*, 36(10), 12210-12213. 876  
877  
878
97. Tsoulos, I. G., Gavrilis, D., & Glavas, E. (2009). Solving differential equations with constructed neural networks. *Neurocomputing*, 72(10-12), 2385-2391. 879  
880  
881
98. Tsoulos, I. G., Mitsi, G., Stavrakoudis, A., & Papapetropoulos, S. (2019). Application of machine learning in a Parkinson's disease digital biomarker dataset using neural network construction (NNC) methodology discriminates patient motor status. *Frontiers in ICT*, 6, 10. 882  
883  
884
99. Christou, V., Tsoulos, I., Loupas, V., Tzallas, A. T., Gogos, C., Karvelis, P. S., ... & Giannakeas, N. (2023). Performance and early drop prediction for higher education students using machine learning. *Expert Systems with Applications*, 225, 120079. 885  
886  
887
100. Toki, E. I., Pange, J., Tatsis, G., Plachouras, K., & Tsoulos, I. G. (2024). Utilizing Constructed Neural Networks for Autism Screening. *Applied Sciences*, 14(7), 3053. 888  
889  
890
101. Gavrilis, D., Tsoulos, I. G., & Dermatas, E. (2008). Selecting and constructing features using grammatical evolution. *Pattern Recognition Letters*, 29(9), 1358-1365. 891  
892  
893
102. Georgoulas, G., Gavrilis, D., Tsoulos, I. G., Stylios, C., Bernardes, J., & Groumpas, P. P. (2007). Novel approach for fetal heart rate classification introducing grammatical evolution. *Biomedical Signal Processing and Control*, 2(2), 69-79. 894  
895  
896
103. Smart, O., Tsoulos, I. G., Gavrilis, D., & Georgoulas, G. (2011). Grammatical evolution for features of epileptic oscillations in clinical intracranial electroencephalograms. *Expert systems with applications*, 38(8), 9991-9999. 897  
898  
899
104. Tzallas, A. T., Tsoulos, I., Tsipouras, M. G., Giannakeas, N., Androulidakis, I., & Zaitseva, E. (2016, November). Classification of EEG signals using feature creation produced by grammatical evolution. In 2016 24th Telecommunications Forum (TELFOR) (pp. 1-4). IEEE. 900  
901  
902
105. Park, J., & Sandberg, I. W. (1991). Universal approximation using radial-basis-function networks. *Neural computation*, 3(2), 246-257. 903  
904  
905
106. Yu, H., Xie, T., Paszczynski, S., & Wilamowski, B. M. (2011). Advantages of radial basis function networks for dynamic system design. *IEEE Transactions on Industrial Electronics*, 58(12), 5438-5450. 906  
907  
908
107. Tsoulos, I. G., Charilogis, V., Kyrou, G., Stavrou, V. N., & Tzallas, A. (2025). OPTIMUS: A Multidimensional Global Optimization Package. *Journal of Open Source Software*, 10(108), 7584. 909  
910  
911
108. Tsoulos, I. G. (2022). QFC: A Parallel Software Tool for Feature Construction, Based on Grammatical Evolution. *Algorithms*, 15(8), 295. 912  
913  
914
109. Chang, C. C., & Lin, C. J. (2011). LIBSVM: A library for support vector machines. *ACM transactions on intelligent systems and technology (TIST)*, 2(3), 1-27. 915  
916  
917

**Disclaimer/Publisher's Note:** The statements, opinions and data contained in all publications are solely those of the individual author(s) and contributor(s) and not of MDPI and/or the editor(s). MDPI and/or the editor(s) disclaim responsibility for any injury to people or property resulting from any ideas, methods, instructions or products referred to in the content.